Characterization of Commercial Al-Si Casting Alloys Reinforced with Nano SiC Composites

Ali Mazahery
Mohsen Ostad Shabani

Materials and Energy Research Center (MERC), P.O. Box 14155-4777, Tehran, Iran

This paper is aimed at studying the microstructure and mechanical properties of nano composites, processed via stir casting. The composites are based on the A356 aluminum alloy, reinforced with nano-SiC particles. The density measurements showed that the samples contained little porosity, and the amount of porosity in the composites increased with increasing volume fraction. The microstructures of composites were examined using optical microscopy (OM) and transmission electron microscopy (TEM). Microscopic observations of the microstructures revealed that the dispersion of the particles was uniform. The tensile strength (yield strength and ultimate tensile strength) and the Young's modulus improve with the addition of nano particles although some reduction in ductility is observed. The highest yield strength and UTS was obtained by 3.5 vol. % of SiC nano-particles. A relatively ductile fracture in tensile fractured samples was observed by fractography examination.

Keywords: Aluminum matrix composites, Silicon carbides, Microstructure fractography, Nanostructures
Received: 15 February 2012, Revised: 23 May 2012, Accepted: 30 May 2012

1. Introduction

During the last two decades a lot of research has been conducted on aluminium matrix composites (AMCs) in commercial laboratories and small businesses. As a result of these activities, many new AMCs applications have been established, and most of these have found insertion within the commercial sector. Important AMCs applications in the aerospace and infrastructure industries have been enabled by functional properties that include high structural efficiency, excellent wear resistance, and attractive thermal and electrical characteristics. Challenging technical issues have been overcome, including compatibility between reinforcement and matrix, affordable primary and secondary processing techniques capable of adequately controlling reinforcement distribution, engineering design methodologies, and characterization and control of interfacial properties [1-8].

The recent investigations found that the incorporation of nano-particles into the aluminum matrix enhance the hardness, yield and ultimate tensile strength considerably, while the ductility is retained [9, 10]. The great enhancement in strength values of these composites was attributed to grain refinement, the strong multidirectional thermal stress at the matrix/nano particle interface, small size of nano particle, good distribution of the nano particles, and low degree of porosity which leads to effective transfer of applied tensile load to the uniformly distributed strong nano particulates. The strength of composites is expected to be influenced by the dislocation density, dislocation-to-dislocation interaction and constraint of plastic flow due to resistance offered by particles. It is reported that due to the thermal mismatch stress, there is a possibility of increased dislocation density within the matrix which lead to making local stress and also increase in strength of the matrix, and thus to the composite. More than 50% improvement in yield strength of A356 alloy was observed only with 2.0 wt. % of nano-sized SiC particles [8]. Zhao et al. [2] characterized the properties and deformation behavior of aluminum matrix nano-composites. It is reported that elongation, ultimate tensile strength and yield strength of nano-composites are enhanced with increasing of particulate volume fraction, and are markedly higher than that of Al composites synthesized by micro size particles.

This paper is aimed at the characterization of microstructure and mechanical properties in commercial Al-Si casting alloys reinforced with nano SiC composites.

2. Experiments

Due to its good castability the aluminium alloy A359, with the chemical composition listed in Table (1), was used as matrix material.

A mixture of nano-SiC and aluminum particles with respectively average particle size of 50 nm and 16 μm was used as the reinforcement. The powders were mixed in the ratio of Al/SiC=1.67 and ball

milled in isopropyl alcohol for 20 min using WC/Co balls. The mixture was then dried in a rotary vacuum evaporator and passed through a 60 mesh screen. The powder mixtures were cold pressed under 200 MPa into samples having 60×60×60 mm^3 dimension. The compacted samples were crushed and then passed through 60 mesh screen. The required amount of SiC was calculated according to the ratio of Al/SiC. Aluminum 356 alloy was selected as the matrix and 1 wt. % magnesium additive in powder form was also used as a wetting agent. Experiments were carried out using a relatively simple experimental set-up which consists of several parts. The main part allows temperatures of up to 1000°C to be reached. This is surrounded by a 50 mm thick layer of kaowool insulator to minimize heat loss. Inside the heater band is a graphite crucible for holding the materials, which has a lid. Weighed quantity of Al-356 alloy was charged into the crucible and heated up to 750^oC (above the alloy liquidus temperature) for melting. There is a nitrogen supply to the crucible in order to minimize the oxidation of molten aluminum, and a graphite stirrer mounted on a graphite shaft passes through small hole out of the crucible lid. This hole also acts as the outlet for the nitrogen gas. The shaft is connected to a digital DC motor used to stir the slurry. The end of the shaft is used to facilitate bottom pouring of the composite melt. During stirring it acts as a plug at the bottom of the crucible and, for pouring, the stirring rod assembly is lifted a distance of 5–10 mm, thus opening the stopper and allowing the slurry to flow into a mould beneath the set-up. This feature is to ensure that the impurities floating on the surface of the melt are not mixed into it.

Table (1) Chemical composition of the aluminium alloy used as matrix

Element	Al	Si	Fe	Cu	Mg
Wt%	Balance	7.2	0.12	0.001	0.33
Element	Mn	Zn	Ti	Ni	
Wt%	0.02	0.02	0.01	0.04	

The powder mixture was inserted into an aluminium foil by forming a packet and added into molten metal of crucible when the vortex was formed. The packet of mixture melted and the particles started to distribute around the alloy sample.

Microstructural evaluations were carried out using optical microscope, scanning electron microscope (SEM) and transmission electron microscope (TEM). Optical microscope and SEM specimens were ground through grit papers and etched with Keller's reagent (2 ml HF (48%), 3 ml HCl (conc.), 5 ml HNO_3 (conc.) and 190 ml water). TEM specimens were machined to 0.5mm thickness and cut using a wire electro discharge machine. The samples were then ground down (350 to 1200 grit) and perforated using double spew with methanol solution. The experimental density of the composites was obtained by the Archimedian method of weighing small pieces cut from the composite cylinder first in air and then in water, while the theoretical density was calculated using the mixture rule according to the weight fraction of the nano particles. The porosities of the produced composites were evaluated from the difference between the expected and the observed density of each sample.

The tension tests were used to assess the mechanical behavior of the composites. The tensile specimens were machined from composite rods according to ASTM.B 557 standard. For each volume fraction of SiC particles, three samples were tested. In order to study the effect of nano-particles on the fracture mechanisms during tensile loading of the samples, fractography was performed on the fractured surfaces of composite specimens. To study the hardness, the Brinell hardness values of the samples were measured on the polished samples using a ball with 2.5mm diameter at a load of 31.25 kg.

3. Results and Discussions

Optical micrographs of unreinforced Al alloy and composites reinforced with SiC particles are shown in Fig. (1). Dendritic microstructure, as the result of casting process is clearly revealed in this figure. This trend was observed in previous works [9,10].

(a)

(b)

Fig. (1) Optical photomicrographs: (a) unreinforced A356 alloy (b) A356 reinforced with 1.5 vol. % SiC

Further study of these composites with high magnification bright field TEM shows the uniform distribution of SiC particles through the matrix alloy (Fig. 2). It is assumed that the uniform dispersion of nano-particles provides some heterogeneous nucleation sites during solidification, resulting in a more refined microstructure. Figure (3) shows the grain morphology results of the composites.

Fig. (2) TEM bright field image of composites with 3.5 vol.% nano-SiC particles

Energy dispersion spectrum (EDS analysis) was utilized to determine the composition of the nano-composite (Fig. 4). The detection zone of EDS beam is bigger than the average size of SiC, therefore the EDS peaks for SiC nano-paricles will inevitably include compositional information of Al matrix near particles. However, according to the compositional information of matrix, it is evident that Si and C peaks correspond to composition of nano-particles.

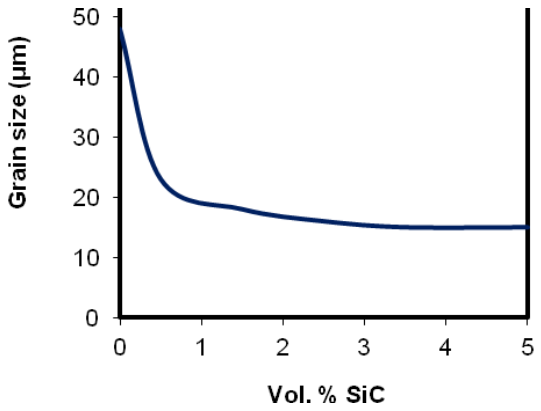

Fig. (3) Results of grain morphology

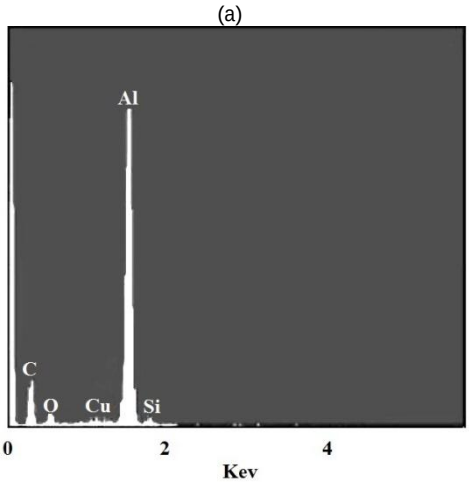

Fig. (4) (a) SEM micrograph and (b) EDS Spectrum of the sample with 2.5 vol. % SiC

Comparison of the measured density of the cast alloy and the composites with that of their theoretical density determined the amount of porosity. Figure (5) shows the variation of porosity with the volume fraction of nano-SiC particles. Higher degree of defects and micro-porosity is observed at higher SiC content which is the result of increase in the amount of interface area [11, 12].

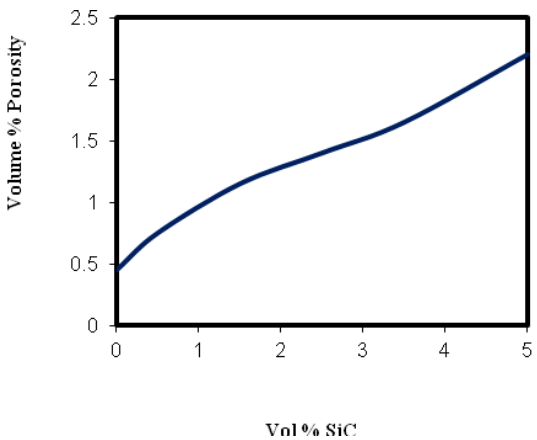

Fig. (5) Variations of porosity with the nano-SiC content

Hardness tests were performed using a Brinell hardness machine. In order to obtain the average

values of hardness, areas predominant in the soft matrix or the hard reinforcing phase should be avoided so that the average values of hardness are attained from these measurements. The variation in hardness with volume fraction for Al/nano-SiC composites are summarized in Fig. (6).

Fig. (6) Variation of hardness as a function of vol.% SiC particulates

It is clear from the graph that the hardness of the composites is higher than that of the non-reinforced alloy. The higher hardness of the composites could be attributed to the fact that SiC particles act as obstacles to the motion of dislocation. The hardness increment can also be attributed to reduced grain size. As shown, hardness increases with the amount of SiC present particles. It is believed that since SiC particles are harder than aluminum alloy, their inherent property of hardness is rendered to the soft matrix [13, 14].

Figures (7), (8) and (9) display the tensile flow curves, yield strength and UTS of the composites, respectively.

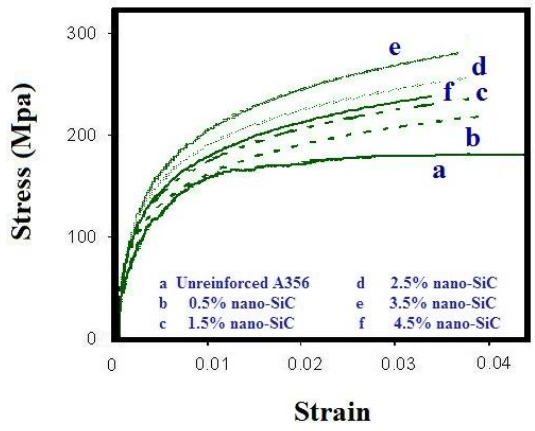

Fig. (7) Flow curves in tensile deformation of the composites

It could be noted that the flow curves do not show any sharp yield point irrespective of the material and the strength values increases with the addition of nano-SiC particles. It is believed that the great enhancement in tensile flow stress observed in these composites is due to good distribution of the nano-SiC particles and low degree of porosity which leads to effective transfer of applied tensile load to the uniformly distributed strong SiC particulates. The grain refinement and strong multidirectional thermal stress at the Al/SiC interface are also important factors, which play a significant role in the high strength of the composites. SiC particles have grain-refined strengthening effect, since they act as the heterogeneous nucleation catalyst for aluminum which is improved with increase in the volume fraction [9-15].

Fig. (8) Variations of yield strength as a function of vol. % nano-SiC particulates

Fig. (9) Variations of UTS as a function of vol. % nano-SiC particulates

The difference between the coefficient of thermal expansion (CTE) values of matrix and ceramic particles generates thermally induced residual stresses and increase dislocations density upon rapid solidification during the fabrication process. The interaction of dislocations with the non-shearable nano-particles increases the strength level of composite samples. According to the Orowan mechanism, the nano-SiC particles act as obstacles to hinder the motion of dislocations near the particles in the matrix. This effect of particles on the matrix is enhanced gradually with the increase of particulate volume fraction [2, 10].

According to the results of this experiment, quite significant improvement in strength is noted initially when particles are added; however, further increase in SiC content leads to reduction in strength values. The weakening factors of mechanical properties

might be responsible for this including particles clusters and porosity. Hereby, it is believed that strengthening and weakening factors of mechanical properties could neutralize the effect of each other and thus, the composite containing 3.5 vol. % SiC exhibits maximum tensile flow stress. Normally micron-sized particles are used to improve the ultimate tensile and the yield strengths of the metal. However, the ductility of the MMCs deteriorates significantly with high ceramic particle concentration [16-18].

It is of interest to use nano-sized ceramic particles to strengthen the metal matrix, while maintaining good ductility [6,19]. It is inferred from Fig. (10) that the addition nano-particles deteriorate the ductility of A356 alloy. The stir casting method that is used in the present work to produce the nano-composites can most probably create different interfaces between nano-particles and matrices and thus, encourage crack initiation and propagation [10]. It is also noted that the elongation remain rather constant with the addition of nano particles. This is consistent with the findings of Hassan and Gupta [20, 21].

Fig. (10) Variations of elongation as a function of vol. % nano-SiC particulates

Fig. (11) SEM fractograph of tensile fracture surface for the composites with 3.5 vol. % nano-SiC particles

Typical SEM micrographs of tensile fracture surfaces for composites are shown in Fig. (9). The tensile fracture surfaces of the samples are clearly indicative of lot of dispersed shallow and small dimples with varying sizes in the matrix, confirming the high ductility observed in the tensile studies. However, there are a number of larger dimples linked together along the boundaries, showing increased degree of clustering along the grain boundaries (Fig. 11).

4. Conclusions

In this research, nano-sized SiC particles were successfully incorporated into the aluminum matrix. Optical microscope examination revealed the grain refining effect of nano-particles. A reasonably uniform distribution of SiC nano-particles in the Al matrix was observed by electron microscopes. Porosity level increased slightly with increasing particulate content which can be attributed to the increased surface area of the nano-SiC particles. The addition of nano-particles resulted in significant improvements in hardness, yield strength and UTS of the composites. Different strengthening mechanisms contributed in the obtained strength improvements including Orowan strengthening, grain refinement, accommodation of CTE mismatch between the matrix and the particles, and the load bearing effects. The dispersed dimples with varying sizes were observed in the fractured surface tensile specimens, confirming the high ductility of the nano-composites.

References

[1] Tu J.P. et al., *Mater Lett*., 2002; 52(6): 448–452.
[2] Zhao Y.T. et al., *Compos. Sci. Technol*., 2008; 68: 1463–1470.
[3] Shabani M.O. and A. Mazahery, *Synthetic Metals*; 161 (2011) 1226–1231.
[4] Ferkel H. and B.L. Mordike, *Mater. Sci. Eng.* A 2001; 298: 193–199.
[5] Akio K. et al., *J. Jpn. Inst. Light Met.* 1999; 49: 149–154.
[6] Shabani M.O. and A. Mazahery, *J. Mater. Sci.*, (2011) 46:6700–6708.
[7] Lan J., Y. Yang and X. Li, *Mater. Sci. Eng.* A 2004; 386: 284–290.
[8] Lan J., Y. Yang and X. Li X, *Mater. Sci. Eng.* A 2004; 380: 378–383.
[9] Mazahery A., H. Abdizadeh and H.R. Baharvandi, *Mater. Sci. Eng*. A 2009; 518: 61–64.
[10] Habibnejad-Korayema M., R. Mahmudia and W.J. Pooleb, *Mater. Sci. Eng.* A 2009;
[11] Suresh K.R. et al., Proc. of the 14th Int. Conf. on Wear of Materials, August–September, 2003, 638.
[12] Hassan S.F. and M. Gupta, *Metallurg. Mater. Trans.*, 2005; 36A: 2253–2258.
[13] Cooke P.S. and P.S. Werner, *Mater. Sci. Eng.* A144 (1991) 189–193.
[14] Mondal D.P., N.V. Ganesh and V.S. Muneshwar, *Mater. Sci. Eng.* 2006; 433: 18–31.
[15] Watson M.C. and T.W. Cline, *Acta Metallurg. Mater.*, 1992; 40: 131–139.

[16] Reddy R.G., *Rev. Adv. Mater. Sci.*, 2003; 5: 121–133.
[17] Kang Y.C. and S.L.I. Chen, *Mater. Chem. Phys.,* 2004; 85(2–3): 438–443.
[18] Hirata Y. et al., *J. Euro. Ceram. Soc.*, 30(9), 2010, 1945-1954.
[19] Mussert K.M. et al., *J. Mater. Sci*., 2002; 37: 789–794.
[20] Hassan S.F. and Gupta M., *J. Mater. Sci.*, 2006; 41: 2229–2236.
[21] Hassan S.F. and Gupta M., *Mater. Sci. Eng.* A 2005; 392: 163–168.